Radiant wall cooling with pipes arranged in insulation panels attached to facades of existing buildings

Martin Šimko[1], *Michal* Krajčík[1,*], and *Ondřej* Šikula[2]

[1]Slovak University of Technology, Faculty of Civil Engineering, Radlinského 11, 810 05 Bratislava, Slovakia
[2]Brno University of Technology, Faculty of Civil Engineering, Veveří 331/95, 602 00 Brno, Czech Republic

Abstract. Radiant systems are being increasingly used for space heating and cooling of buildings. The contemporary research of radiant systems addresses mainly floor and ceiling structures. Research regarding the possibilities of their incorporation in wall structures is lacking, despite their potential advantages. This study addresses a radiant wall system manufactured according to a patent. The patented design involves panels that consist of pipes arranged in milled channels in thermal insulation. The potential advantage of this system is the fact that the thermally active panels can be attached to the facades of existing buildings as a part of their retrofit. Thereby, only minor interventions on the interior side of the retrofitted buildings are needed. To test and improve the design of the wall system, laboratory measurements and computer simulations were performed on a wall fragment for its operation under summer conditions. The results indicate a significant potential for improvement of the patented design by addressing the imperfections in the contact between pipe and wall. Inserting a metal fin between pipe and wall enhanced the cool distribution within the wall fragment considerably. From the three materials of the metal fin considered, using copper led to highest values of the cooling output, followed by aluminium. For these two metals the effect of increasing the thickness of the fin on the cooling output was small. On the contrary, the fin made of steel was the least efficient in terms of cool distribution. In this case the cooling output was most sensitive to the thickness of the fin.

1 Introduction

Current trends in the design and operation of heating, ventilation and air conditioning include the increasingly frequent use of low-exergy water-based radiant systems. Installation of such systems can be beneficial due to their suitability for combination with low-grade renewable energy sources such as ground-coupled heat pumps and solar collectors [1,2], the high sensible cooling capacity [3], and the possibility to use the same system both for heating and cooling [4-6].

Although research on radiant surfaces has been mostly focused on structural floors and ceilings, evidence from several research studies suggests that radiant walls also present a potentially feasible solution for space heating and cooling [7-9]. Nevertheless, scientific studies related to radiant wall systems are relatively scarce, and research regarding the potential of their installation in existing buildings as a part of retrofit is lacking.

In this study we explore the potential of a wall cooling system constructed according to a patent [10]. The patented design involves pipes arranged in milled channels in thermal insulation, whereby panels are formed. The potential benefit of this system is the possibility to attach the panels to the facades of existing buildings as a part of their retrofit so that only minor interventions on the interior side of the retrofitted buildings are needed. The system can be operated both as space cooling in summer and as space heating in winter. Moreover, it can potentially serve as a thermal barrier to reduce transmission heat losses in winter and heat gains in summer. This is possible in situations when the water temperature is very close to the room temperature, thus preventing heat losses in winter [11,12] and absorbing external heat gains in summer [13].

Numerical simulations and experiments were employed to explore details of the heat transfer within a wall fragment manufactured in accordance with the patent [10]. The investigations refer to the operation as space cooling under summer conditions. Subsequently, the possibilities to enhance cool distribution within the wall fragment by inserting a metal fin between pipe and wall were researched by numerical simulations.

2 Laboratory measurements and computer simulations of heat transfer through the wall

The results of laboratory measurements and computer simulations are presented for operation of the wall system as space cooling under summer conditions. The laboratory measurements were also used for validation of the computer simulations.

* Corresponding author: michal.krajcik@stuba.sk

2.1. Measurement of the heat transfer

The laboratory measurements were performed on an experimental wall fragment. The wall fragment consisted of cooling pipes embedded in milled channels in thermal insulation made of polystyrene, attached to the concrete core in the form of panel. The dimensions of the fragment were 1140 mm x 1360 mm (Fig. 1). The calculated heat transfer coefficient of the wall was 0.35 W/(m^2.K). The temperature of the concrete was monitored by PT100 platinum resistance thermometers with the accuracy variable in the range of ±0.15°C, located at selected points along the panel (points A, B, C, D in Fig. 1) at several depths (points 1 to 5 in Fig. 1). Supply and return water temperature was also recorded. The heat flux was monitored by a thermopile sensor for studies of the radiative and convective heat flux with a level of accuracy variable in the range ±5% of the value measured. The sensor was located underneath the surface in the centre of the fragment as recommended by Ref. [14].

The wall was located between two climate chambers with controlled air temperature and humidity (Fig. 2). The fragment was exposed to the air temperature of 32°C simulating ambient conditions on one side, and to the air temperature of 26°C simulating the room conditions on the other side. Direct solar radiation was not considered in this study. The temperature of the supply water was kept constant at about 18°C. The temperature of the inlet air was adjusted to obtain the desired air temperature in each of the two chambers. The heat transfer coefficients between the surface of the wall and each chamber were calculated by a CFD simulation in ANSYS Fluent.

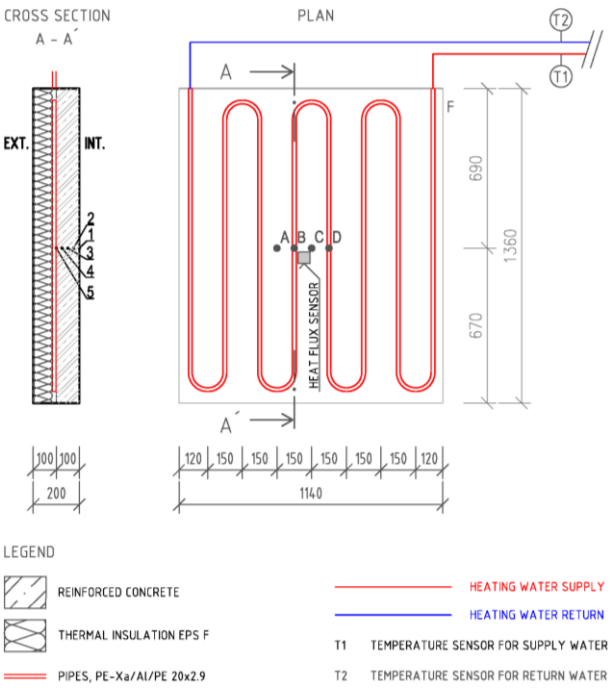

Fig. 1. Details of experimental wall with location of sensors

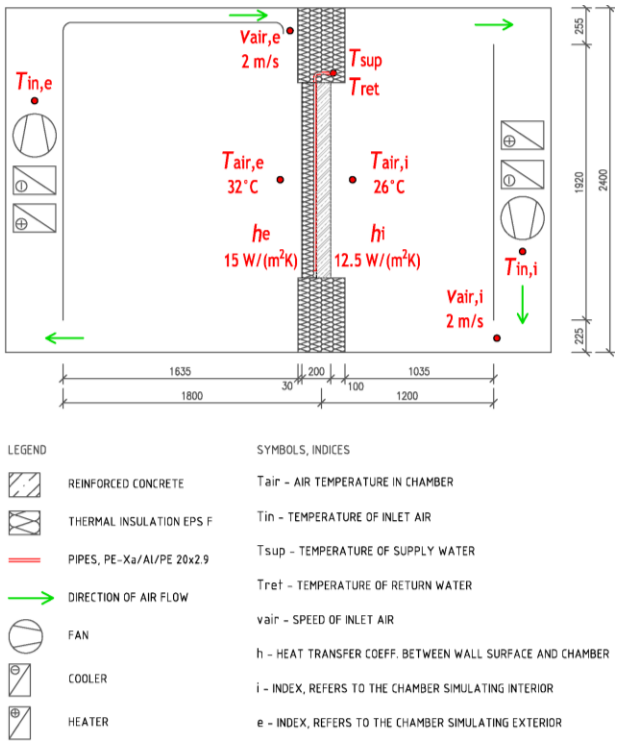

Fig. 2. Cross section of experimental chambers and location of sensors

2.2. Heat transfer coefficients between wall and room

We used computer simulations in ANSYS Fluent software to visualize the air temperature and velocity fields and calculate the heat transfer coefficients between wall surface and room. Each of the chambers was simulated individually. The boundary condition assigned at the inlet was: velocity inlet (2 m/s) and turbulence intensity (5%), with equivalent hydraulic diameter. The boundary condition assigned at the outlet was: pressure outlet. Newton-Robin boundary condition was assigned at the wall´s surface, with the virtual temperature (T) taking the value 18.6°C and the thermal resistance at heat conduction from the virtual temperature to the surface (R) taking the value 5 (m^2.K)/W. The heat transfer coefficient at the wall´s surface depends primarily on forced convection. To obtain a reliable value of the heat transfer coefficient, keeping the correct difference between the temperature of the surface and the ambient temperature was crucial. Assigning exact values of T and R had only secondary effect on the calculation accuracy. Some uncertainty in T and R was therefore allowed.

Fig. 3 shows the results of CFD simulations for the chamber simulating interior. The air flow pattern resulted in the air velocity higher at the wall surface than in the rest of the chamber (Fig. 3a). Consequently, the heat transfer coefficient at the inner wall was higher than the 8 W/(m^2.K) recommended for the design of radiant wall systems [15]. Although the heat transfer coefficients fluctuated over time, the value 12.5 W/(m^{2}K) was determined as representative (Fig. 3b). For the chamber simulating exterior the heat transfer coefficient was determined to 15 W/(m^2.K).

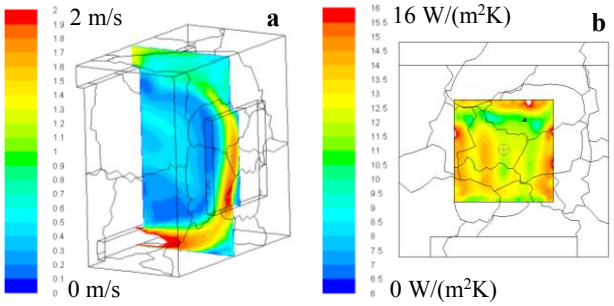

Fig. 3. Results of CFD simulation in the chamber simulating indoor environment: a) air velocity profile, b) heat transfer coefficient between wall surface and chamber

2.3. Calculation of the heat transfer

The results were obtained by solving a set of equations of two-dimensional heat transfer by conduction, using a dedicated CalA software [16,17], which has been validated in accordance with [18]. The calculation was based on a detailed numerical solution of two-dimension stationary temperature field by the method of rectangle-shaped control volumes, each representing a single temperature [19]. The distribution of the temperature in the Cartesian coordinate system was described by the Fourier equation of thermal diffusion [20]:

$$\frac{\partial}{\partial x}\left(\lambda\frac{\partial T}{\partial x}\right)+\frac{\partial}{\partial y}\left(\lambda\frac{\partial T}{\partial y}\right)+S=\rho.c.\frac{\partial T}{\partial \tau} \qquad (1)$$

where T is the temperature (K); S is an internal heat source (W/m^3); τ is time (s); λ is thermal conductivity (W/(m.K)); ρ is bulk density (kg/m^3); and c is the specific heat capacity at a constant pressure (J/(kg.K)).

The heat transfer coefficient for the water and pipe surface α was determined to be 1218 W/(m^2.K). The boundary conditions defining the specific heat flux on the surface of a computational domain were calculated according to the Newton's law of cooling, assuming adiabatic boundaries of the wall fragment (Fig. 4). The temperature and heat flux distribution over time was calculated using the Robin-Newton´s boundary condition.

The simulated fragment represented a section of radiant wall, symmetrical along the horizontal axis. The pipes in the radiant wall were spaced regularly and the temperature of the water in the pipes and material properties were considered homogeneous along the wall.

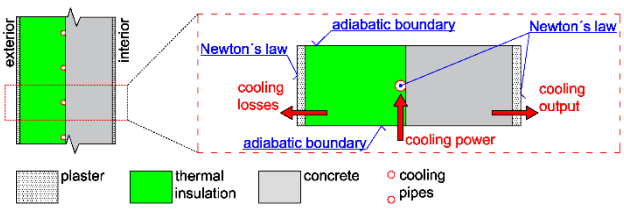

Fig. 4. Boundary conditions defining specific heat flux on a wall surface.

2.4 Results

Fig. 5 shows the values of air temperature measured in the chambers simulating the indoor (θ_i) and the outdoor environment (θ_e) and compares the experiments with the results of dynamic simulations in CalA software. In the simulations, measured data were used as the input regarding air temperature. The inputs regarding heat transfer coefficients were obtained by CFD simulations in ANSYS Fluent as described in 2.2. The volumetric weight of the reinforced concrete and the heat transfer coefficient between pipe and wall were adjusted to fit the results of simulations on the experimental data. Very good agreement was achieved between simulations and experiments regarding heat flux and surface temperature at the point C1 (see Fig. 1). The cooling output was relatively low, about 7 W per m^2 of wall surface.

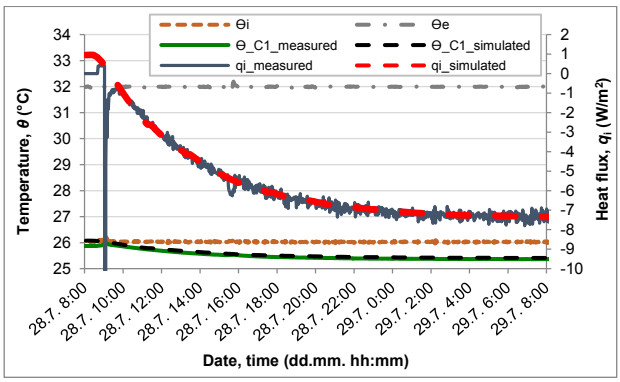

Fig. 5. Comparison of temperature and heat flux obtained by measurements and simulations

2.5 Heat transfer between pipe and wall

The low values of heat flux were attributed to imperfections in the contact between pipe and wall. In the computer simulations of heat transfer in CalA software (Fig. 5), these imperfections were approximated by an air gap between pipe and thermal insulation. In order to fit the simulations on experimental data, an equivalent heat transfer coefficient between pipe and wall (h_{equiv}) was defined (Fig. 6a). This coefficient takes into account the heat transfer between water and pipe (h_{water}), equal to 1218 W/(m^2.K), and also the hindering effect of the imperfect contact between pipe and wall. The effect of imperfections, simulated by the air gap, can be expressed by an additional heat transfer coefficient between pipe and its surrounding (h_{gap}), calculated from eq. 2 (Fig. 6b).

$$h_{equiv} = 1 / (1/h_{gap} + 1/h_{water}) \qquad (2)$$

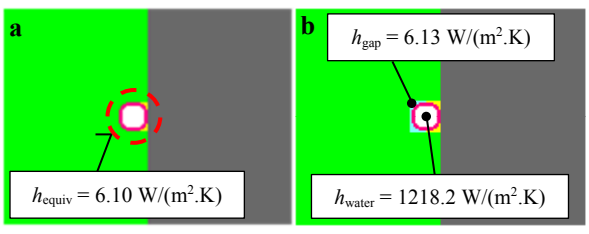

Fig. 6. Heat transfer between pipe and wall: a) equivalent heat transfer coefficient, b) heat transfer coefficients between water and pipe (h_{water}), and between pipe and its surrounding (h_{gap})

3 Optimization of the cooling output

The simulations and experiments proved that imperfections in the contact between pipe and wall can hinder the heat transfer considerably. In the following sections we therefore investigate the possibilities to improve the patented solution [10] with the aim to find feasible designs to enhance the cooling output.

3.1. Physical model and boundary conditions

The possible enhancements of the cooling output were researched by stationary simulations performed by CalA software in accordance with the calculation principle as described in 2.3. Fig.7 shows the simulation model as defined in CalA. The thermo-physical properties of the individual material layers are summarized in Table 1.

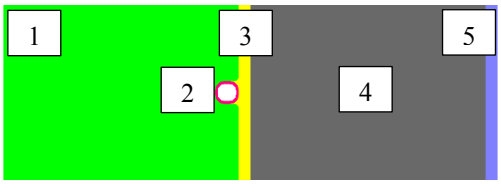

Fig. 7. Physical model of wall fragment as defined in CalA

Table 1. Thermo-physical properties of the material layers.

No.	Material	Thickness m	Vol. weight kg/m³	Thermal conductivity W/(m.K)	Specific heat capacity J/(kg.K)
(1)	Insulation - EPS F	0.02	17	0.04	1270
(2)	Plastic pipe DN 20	--	1200	0.35	1000
(3)	Plaster between pipe and concrete	0.01	1300	0.8	840
(4)	Reinforced concrete	0.2	2400	1.58	1020
(5)	Inner plaster	0.01	1600	0.88	840

The results presented in this section refer to the room temperature of 26°C, which is interpreted as the operative temperature [21], and the mean temperature of cooling water of 21°C, considered as typical for radiant cooling systems operated in temperate climates. The total heat transfer coefficient (h_i) between the radiant surface and the space was 8 W/(m^2.K), and the heat transfer coefficient for the water and pipe surface was 1218 W/(m^2.K). The combined effect of ambient temperature and solar radiation incident on the wall was approximated by the sol-air temperature ($T_{sol\text{-}air}$) [20]:

$$T_{sol-air} = T_{amb} + \frac{\alpha . I_g}{h_e} \quad (3)$$

where T_{amb} is the temperature of the ambient air, equal to 30°C; α is the absorptance of surface for solar radiation, equal to 0.9; I_g is the solar radiation incident on the wall, equal to 450 W/m^2; h_e is the coefficient of heat transfer by long-wave radiation and convection at outer surface, equal to 15 W/(m^2.K). The sol-air temperature, $T_{sol\text{-}air}$, was determined to 57°C.

3.2. Enhancement of the cooling output

The improvements to enhance the cooling output are represented by inserting a metal fin between pipe and thermally conductive plaster. The purpose of the fin is to efficiently distribute the cool from the pipe to the thermally conductive plaster. Fig. 8 illustrates the difference in the cooling output between a wall fragment without any fin (a) and with a fin with the thickness of 1.56 mm, made of copper (b). Adding the metal fin enhanced the cooling output by about 50%.

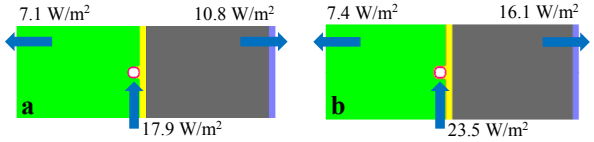

Fig. 8. Cooling power, output, and losses of a wall fragment: a) without metal fin, b) with metal fin made of copper, thickness of 1.56 mm, thermal conductivity λ = 372 W/(m.K)

The distribution of temperature and cooling output for the wall fragment with and without any metal fin is visualised in Fig. 9. The metal fin between pipe and plaster improved the distribution of cool within the wall. This is illustrated by the larger (dark blue) area with cooler temperature between pipe and interior (Fig. 9a) and by the homogeneous distribution of heat flux in the case with metal fin (Fig. 9b).

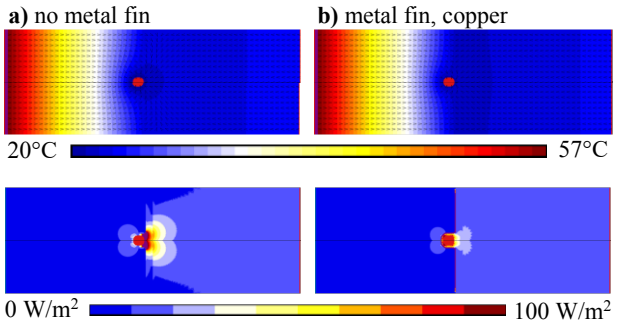

Fig. 9. Distribution of temperature (°C) and heat flux (W/m^2) within the wall fragment: a) without metal fin, b) with metal fin

To find out the most feasible design, it is crucial to know the effect of material and thickness of the fin on the cooling output. Fig. 10 shows comparison of the heat flux to the interior, i.e. the cooling output, for the fin made of three different materials – copper (q_{i_Cu}), aluminium (q_{i_Al}), and steel (q_{i_steel}). Five cases were considered for the solution with the fin made of copper which was most efficient in terms of cool distribution. Three cases were considered for both aluminium and steel to allow comparison. The difference between the fins made of aluminium and copper was small regardless of its thickness. Increasing the thickness of the fin had only minor effect on the cooling output. Fin made of steel was the least efficient. In this case the cooling output was most sensitive to the thickness of the fin.

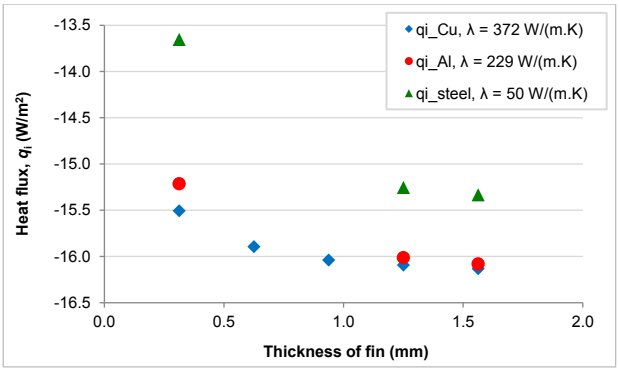

Fig. 10. Cooling output of wall fragments with variable thickness and materials of the fin

4 Conclusion and recommendations

We explored details of the heat transfer within a wall fragment manufactured in accordance with a patent [10] under summer conditions. Subsequently, we researched the possible improvements of the design to enhance the cooling output. The conclusions that may be drawn from this study are:

- The potential for improvement of the patented design is substantial. It was found that the cooling output can be enhanced by addressing the imperfections in the contact between pipe and wall. Inserting a metal fin between pipe and plaster has improved the cool distribution within the wall fragment considerably.
- From the three materials of metal fin considered, using copper led to highest values of cooling output, followed closely by aluminium. The cooling output of the fin was increasing with its thickness, however, for copper and aluminium the effect of fin thickness on the cooling output was relatively small. On the other hand, fin made of steel was the least efficient in terms of cool distribution. In this case the cooling output was most sensitive to the thickness of the fin.
- In future research other designs should be considered such as, for example, embedding the pipe in a thermally conductive plaster. This could be a potentially feasible solution because the associated costs might be lower than in the case of metal fin. Moreover, the design of the fin could be potentially improved by using grooved instead of smooth surface.

This work was supported by the Slovak Research and Development Agency under the Contract No. DS-2016-0030 and under the Contract No. APVV-16-0126, by the Ministry of Education, Science, Research and Sport of the Slovak Republic under VEGA Grant 1/0807/17, and by the Brno University of Technology Project No. FAST-J-19-5976 “Optimization of thermally activated structures”.

References

1. U. Akbulut, O. Kıncay, Z. Utlu. *Analysis of a wall cooling system using a heat pump*. Renew Energ **85** (2016).
2. A.A. Márquez, J.M.C. López, F.F. Hernández, F.D. Muñoz, A.C. Andrés. *A comparison of heating terminal units: Fan-coil versus radiant floor, and the combination of both*. Energy Build **138** (2017).
3. J. Babiak, B.W. Olesen, D. Petráš. *Low temperature heating and high temperature cooling*. Rehva Guidebook No 7. 3rd revised ed. Brussels, Belgium: Rehva (2013).
4. N. Harmati, R.J. Folić, Z.F. Magyar, J.J. Dražić, N.L. Kurtović-Folić. *Building envelope influence on the annual energy performance in office buildings*. Therm Sci **20** (2016).
5. D. Petráš, M. Krajčík, J. Bugáň, E. Ďurišová. *Indoor Environment and Energy Performance of Office Buildings Equipped with a Low Temperature Heating / High Temperature Cooling System*. Adv Mater Res **899** (2014).
6. X. Wu, L. Fang, B.W. Olesen, J. Zhao, F. Wang. *Comparison of indoor air distribution and thermal environment for different combinations of radiant heating systems with mechanical ventilation systems*. Building Serv. Eng. Res. Technol. **39** (2018).
7. H. Karabay, M. Arici, M. Sandik. *A numerical investigation of fluid flow and heat transfer inside a room for floor heating and wall heating systems*. Energy Build **67** (2013).
8. J.A. Myhren, S. Holmberg. *Flow patterns and thermal comfort in a room with panel, floor and wall heating*. Energy Build **40** (2008).
9. M. Bojić, D. Cvetković, V. Marjanović, M. Blagojević, Z. Djordjević. *Performances of low temperature radiant heating systems*. Energy Build **61** (2013).
10. D. Kalus, P. Páleš, Ľ. Pelachová. *Self-supporting heat insulating panel for the systems with active regulation of heat transition*. Patent WO/2011/146024, 2011.
11. M. Krzaczek, Z. Kowalczuk. *Thermal Barrier as a technique of indirect heating and cooling for residential buildings*. Energy Build **43** (2011).
12. M. Šimko, M. Krajčík, O. Šikula, P. Šimko, D. Kalús *Insulation panels for active control of heat transfer in walls operated as space heating or as a thermal barrier: Numerical simulations and experiments*. Energy Build **158** (2018).
13. J. Xie, Q. Zhu, X. Xu. *An active pipe-embedded building envelope for utilizing low-grade energy sources*. J Cent South Univ **19** (2012).
14. Á. Lakatos. *Comprehensive thermal transmittance investigations carried out on opaque aerogel insulation blanket*. Mater. Struct. **50** (2017).
15. EN ISO 11855-2:2012. Building environment design - Design, dimensioning, installation and control of embedded radiant heating and cooling systems - Part 2: Determination of the design heating and cooling capacity.
16. O. Šikula. Software CalA User Manual (In Czech). Brno, Czech Republic: Tribun (2011).

17. J. Plasek, O. Šikula. *Transient numerical simulation of linear thermal transmittance in software CalA*. Adv Mater Res **1041** (2014).
18. EN ISO 6946:2017. Building components and building elements - Thermal resistance and thermal transmittance - Calculation methods.
19. S.V. Patankar. *Numerical Heat Transfer and Fluid Flow*. New York, USA: Hemisphere Publishing Corporation, Tailor & Francis Group (1980).
20. ASHRAE. *ASHRAE Handbook – Fundamentals*. Atlanta, GA, USA: American Society of Heating, Refrigerating, and Air Conditioning Engineers (2017).
21. EN 15251:2007. Indoor environmental input parameters for design and assessment of energy performance of buildings addressing indoor air quality, thermal environment, lighting and acoustics.